

Aerodynamics Simulation of Public Bus Using CFD to reduce Drag and Fuel Consumption

Kshitij Bhandari, Prabin Shakya, Dr. Krishna Prasad Shrestha

Department of Mechanical Engineering, Kathmandu University, Dhulikhel, Kavre, Nepal

Corresponding Author: Kshitij Bhandari

ABSTRACT: Public bus transportation is a comparatively cheaper and accessible means of transportation. There have been great attempts to make the buses even more reliable, efficient, and comfortable. However, it seems the aerodynamic aspect of the buses has been neglected. This paper casts light on the effect of aerodynamic drag on the vehicle's performance. Besides, it is an attempt to minimize fuel consumption rate by reducing drag force acting on the bus with slight modification on its outer-shape. Higer 41-seater bus is selected for the study. The drag analysis of its CAD model in CFD software depicted its drag coefficient to be 0.669. Secondly, retaining the Higer bus as a base model, 3 new modified models are formed and individual drag analyses are carried out for each model. The model with the least drag coefficient of 0.5508 is selected for comparison. It is found that the drag coefficient was reduced by 17.67%. Moreover, after comparison, it has been found that fuel consumption in the fourth model got reduced by around 16.65%. Overall, it is found that even public buses have to tackle with a fair amount of air drag and considerable amounts of fuels are being used to overcome it. The results exhibit that even small changes on today's bus exterior can help them to tackle air drag much effectively. Thus, reducing fuel consumption, which is better from economic as well as environmental point of view.

KEY WORDS: ANSYS, CFD, Aerodynamic drag, 3D CAD model, Fuel Consumption

Date of Submission: 07-08-2020

Date of acceptance: 21-08-2020

I. INTRODUCTION

Aerodynamics is the study of the motion of air and its interaction on solid objects. Aerodynamics is primarily concerned with the force of lift and drag, which are caused by air passing over and around solid objects or bodies [1]. Air drag is a critical factor for determining fuel consumption when the vehicle is moving at a high speed. The aerodynamical shape of the car uses approximately 3% of fuel to resist the drag force in urban driving, while it uses 11% of fuel during the highway driving [2]. At high speeds, about 100 km/hr, the drag force exceeds the power spent on overcoming the rolling resistance. About 90% of drag is due to the pressure difference created in different regions of the vehicle [3].

In the early '70s, the 1st step was taken for the aerodynamics in the production cars because of an increase in fuel prices. A lot of research and investigation have also been made in aerodynamic simulation of a public vehicle like a bus in the world. H. Yesfalgn Damissie and N. Ramesh Babu [4] modified the outer surface of the bus aerodynamically to reduce the effect of the drag force of the bus which in turn results in the reduction of fuel consumption of the bus. E. Mohamed [5] made a study to reduce the gas emissions from buses by reducing the aerodynamic drag. He analyzed six different cases by changing the external body and a computational model was applied. It was found that the reduction in aerodynamic drag up to 14% which corresponds to an 8.4% reduction in fuel consumption. Similarly, S. Thorat, G. Amba, and P. Rao [6] redesigned an intercity bus with enhanced exterior styling reduced aerodynamic drag and CFD was used to evaluate the performance. The results showed a reduction of Cd from 0.581 to 0.41 at a speed of 100 km/hr and overall aerodynamic drag reduction by about 30% due to the combined effect of reduced Cd and frontal area.

Air drag may be a negligible factor for city buses; however, it is a significant factor for highway buses cruising at high speeds. In the context of Nepal, the long route buses travel at high speeds quite constantly, but aerodynamics is not taken into consideration while designing them i.e. the public buses are almost similar to the same design. Buses with effective aerodynamic design are very much expensive. An underdeveloped country like Nepal cannot afford for public use. We, therefore, decided to initiate this project to design an aerodynamic body for the bus making a small improvement in its exterior body, thus reducing the air drag and improving the

fuel economy. This paper puts its major focus on aerodynamics analysis of the public bus to minimize the drag coefficient acting on the bus by minimizing the pressure difference acting on the bus body. Moreover, it extends its study on the impact on the fuel consumption of a vehicle due to the reduction of the drag coefficient followed by the drag force. A 3D CAD design of existing and modified bus models was created in solid works, an analysis was made in ANSYS Fluent, and the obtained results were compared and the modified model with reduced drag coefficient was selected for comparison with the existing model. Some ideal assumptions that were made in this study are:

- Drag force was taken into consideration while other forces like lift, thrust were neglected.
- Friction between road surface and tires was neglected.
- The average speed of the bus at 80km/hr. Since the drag coefficient is directly proportional to the velocity of the bus, thus velocity test for other values of velocity was not performed.

II. METHODOLOGY

Two types of aerodynamic forces act on a vehicle during its motion i.e. aerodynamic drag and aerodynamic lift. The study puts the main focus on drag force only.

2.1 DragForce[7]

Two types of drag force act on the moving body: friction drag and pressure drag. The total drag force is the mathematical addition of pressure drag and friction drag.

Pressure drag: Pressure drag is due to the difference of pressure between the front and rear end of the bus. The pressure drag is created when the shape of the bus surface changes abruptly at the front and rear end. Pressure drag plays a major role in total drag. The pressure drag coefficient can be calculated as:

$$C_{dp} = \frac{\Delta P}{0.5 \times \rho \times v^2} \dots \dots \dots (1)$$

And the pressure drag force can be calculated as:

$$F_{dp} = C_{dp} \frac{\rho v^2}{2} \times A_F \dots \dots \dots (2)$$

Friction/Skin Drag: Friction drag is due to friction between the fluid and moving object. It is created in the boundary layer due to the viscosity of a fluid. Skin drag can be as:

$$C_{df} = \frac{0.031}{Re^{\frac{1}{7}}} \dots \dots \dots (3)$$

And friction drag force can be calculated as:

$$F_{df} = C_{df} \frac{\rho v^2}{2} A_s \dots \dots \dots (4)$$

Where:

C_{df} is the friction drag coefficient

C_{dp} is the pressure drag coefficient

ρ is the fluid density(air)

v is the velocity of the bus in m/s

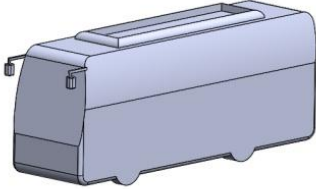
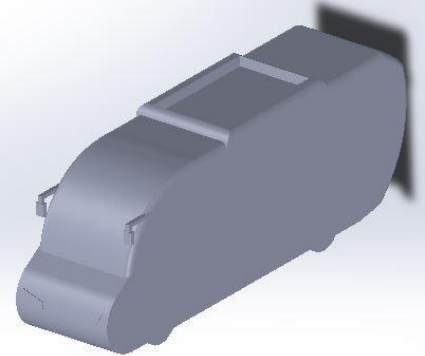
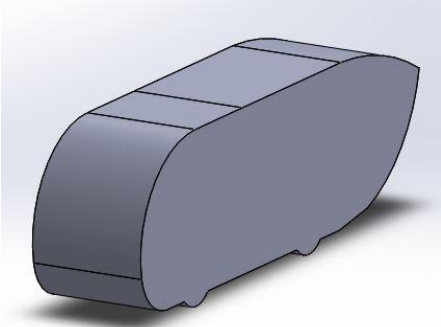
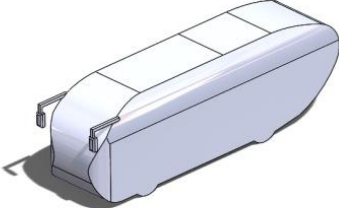
A_s is the total surface area of the bus in contact with the fluid

A_F is the area of the frontal surface of the bus at which airstrikes.

2.2 3D CAD Modelling

To perform aerodynamics analysis, we need to have a 3D model of a bus. A 41-seater Higer bus model was used as a reference design. Three different modified designs were made and all of them were designed benchmarking the higer bus model. Each model has a similar dimension, but in terms of exterior body styling and appearance, they are slightly different when compared to each other. The designs were made in such a way that they help to improve the drag force reduction. All the 3D models are shown in the following table.

Table 1 Name and views of existing and modified bus 3D Model

| S.N | Model | Views |
|-----|----------|--|
| 1 | Existing |  |
| 2 | Second |  |
| 3 | Third |  |
| 4 | Fourth |  |

The models and their views are explained below.

Existing: It is the first model without any modifications. 41-seater Higer bus is taken as reference. It has length, breadth, and height of 8.95m, 2.45m, and 3.36m respectively.

Second: The second model has a protruded nose making a place for the engine as well as the cabin, plus it reduces the pressure at the front face, tapering towards the rear end to provide better-streamlined flow.

Third: The third model has a curved front as well as a curved rear part. Rearview mirrors are removed to be replaced by cameras. The front curve in addition to the rear curve helps to reduce the pressure drag.

Fourth: The fourth model has an additional side taper at the front as compared to the third model further reducing the pressure drag. Finally, hoods have been removed from the third and fourth modelsto further reduce air resistance.

2.3 Simulation on CFD software

After the solid modeling, the CAD model was imported in ANSYS to carry out further processing. The following sequence of methods was followed to carry out CFD analysis.

Geometry:

The 3D model made in CAD software was imported and an enclosure was designed. The enclosure is the volume that encompasses the bus body. The airflow is simulated in this very volume. During this process, the enclosure is created and then the bus body is subtracted so that the air flows around the bus and specific names were given to each subtracted parts as shown in fig below to facilitate boundary condition settings. To reduce the overall computational cost and time, the bus was considered symmetric laterally. The size of the enclosure was taken to be 2 times bus length each: ahead of the bus, above the bus, and beside the bus, whereas 4 times bus length spacing was left at the rear part of the bus.

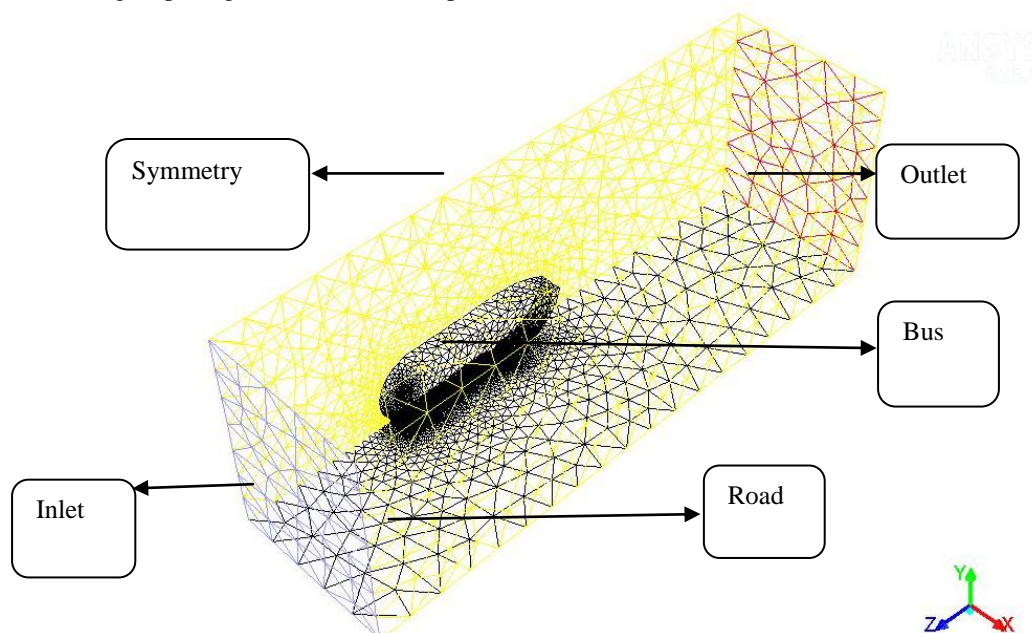


Figure 1 Named selections

Meshing

Meshing is the process of discretizing a model into several elements. It is one of the most important steps in FEA analysis. The accuracy of the result depends on the quality of the mesh.

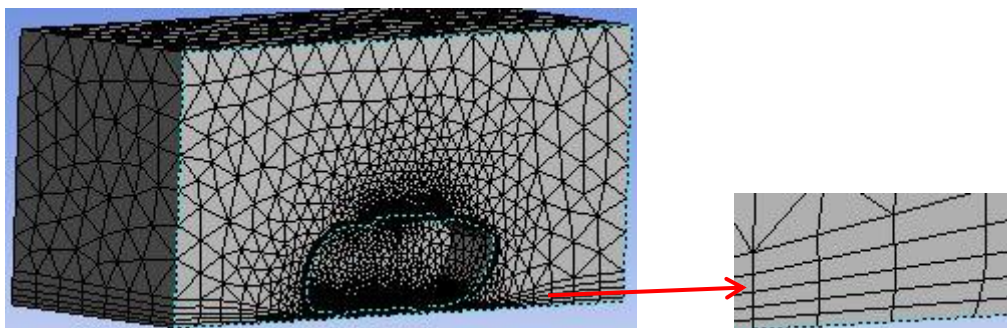


Figure 2 Meshing

Meshing with the following specifications is used in this study with slight adjustment and editing to fit every model geometry and dimension.

Relevance center: Coarse

Skewness: 0.9

Advance sizing function: On proximity and curvature

Inflation: Program controlled with 5 number of layers.

Transition: Slow

Growth rate: 1.2

Face and body sizing: Face sizing of 40mm was given to the faces of the bus body. Similarly, body sizing of 80mm was given to the bus box that was created around the bus body in geometry to make the mesh more refined around the body to capture flow features more accurately. A tetrahedral mesh was converted into the polyhedral mesh for further operation because of its less computational time and faster convergence properties.

Mesh independent test

For the mesh independent test, the element size of minimum 10mm, 20mm, and then 30 mm is taken and tested. Results obtained are shown below;

Table 2 Mesh Independent Test

| S.N. | Minimum element size | Maximum element size | Skewness | Number of elements |
|------|----------------------|----------------------|----------|--------------------|
| 1. | 10mm | 400mm | 0.916 | 3.71 million |
| 2. | 20mm | 800mm | 0.917 | 1.64 million |
| 3. | 30mm | 1000mm | 0.991 | 1.42 million |

Since the mesh quality with 10mm and 20mm gave similar results but smaller element size took more calculation time hence minimum element size of 20mm was used for further processing.

Setup

In this process, fluent is launched after selecting suitable options like single precision and serial processing. The following steps were performed under the setup process.

Pressure based solver was used because the flow is incompressible. Similarly, the steady-state condition was used because the transient is complex and it is used only when steady simulation cannot solve simulation.

Models: Realizable $k-\epsilon$ model and non-equilibrium wall functions were used. Because non-equilibrium wall function performs better for pressure gradient and gives good flow separation[8]. Similarly, the realizable $k-\epsilon$ model captures the mean flow of complex structures.

Boundary conditions: The analysis is carried out with a velocity of 80km/hr. The vehicle was kept stationary, and the air is allowed to flow around the vehicle at vehicle speed. All the boundary conditions applied are shown in table 3.

Table 3 Surface name and boundary conditions

| Surface name | Boundary condition | Values |
|--------------|---------------------------------------|---|
| Road | No-slip stationary wall | |
| Inlet | Constant velocity inlet | Velocity(V)= -22.22m/s (direction opposite to movement of bus) Turbulence intensity=1% |
| Outlet | Constant pressure outlet | Pressure= 0Pa |
| Symmetry | Stationary wall | Shear stress= 0 |
| Bus | No-slip condition and stationary wall | |

Solution

Solution methods: pressure-velocity coupling

Scheme: Coupled

Gradient: Least square cell-based

Pressure: Standard

Momentum & Turbulent KE: Second order upwind

Monitors: Drag coefficient

Final solutions for each model were obtained by performing iterations on the velocity at 80 km/hr. This is the final stage for analysis after inserting all the necessary boundary conditions and set up. The solution is initialized

with hybrid initialization for 10 quick iterations with a laminar model. It would not predict the accurate results but fill the domain with the realistic distribution of pressure and velocity. To predict the accurate results, 400 iterations were set up and the program started to calculate the values of the drag coefficient. Iterations were stopped when the value of the drag coefficient starts to converge.

III. RESULTS AND DISCUSSIONS

The results obtained from the computational study were shown in this section. Velocity tests for all bus models were performed and compared. Similarly, computation of pressure contour, velocity contour, and streamlines around the bus body and their comparisons were made.

Velocity test

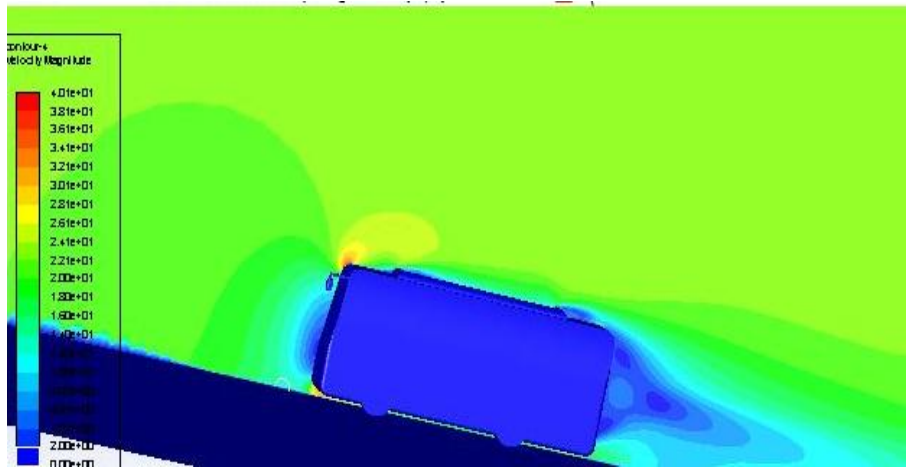
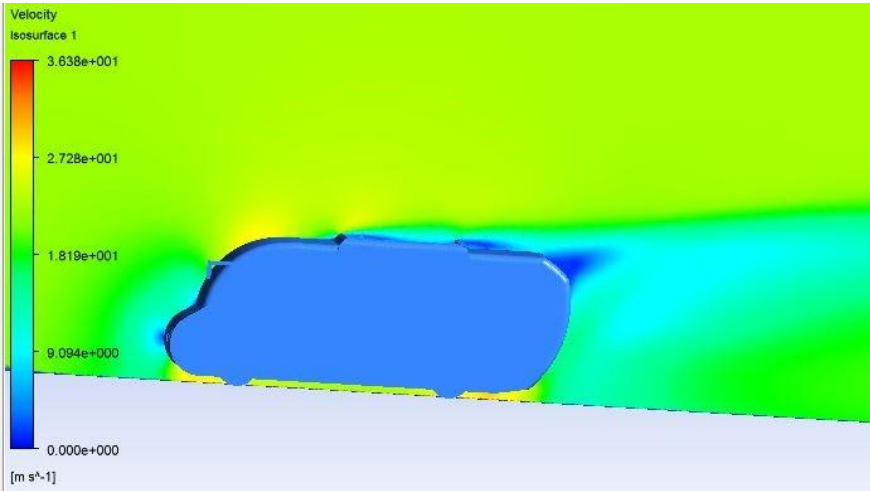
Existing and modified models were tested in the same velocity i.e. at 80 km/hr. The results obtained are depicted below.

Table 4 Velocity test

| S. N | Model | Velocity(m/s) | Drag coefficient (Cd) | Drag Force(N) |
|------|----------|---------------|-----------------------|---------------|
| 1 | Existing | 22.22 | 0.6690 | 1795.38 |
| 2 | Second | 22.22 | 0.6575 | 1742.58 |
| 3 | Third | 22.22 | 0.5966 | 1659.82 |
| 4 | Fourth | 22.22 | 0.5508 | 1496.38 |

Drag force values for all modified models were reduced compared to the existing model. The fourth model gave minimum possible drag force, hence it is used for further calculations. Contours of velocity for existing and modified models were shown below.

Table 5 Contour of the velocity of existing and modified bus models

| S.N | Model | Velocity contour |
|-----|----------|--|
| 1 | Existing |  |
| 2 | Second |  |

| | | |
|---|--------|--|
| 3 | Third | |
| 4 | Fourth | |

The existing model has a square back geometry which is not very helpful in controlling drag as a drastic change in the profile aids boundary layer separation contributing to vortex formation and increase in drag. In all three new models (second, third, and fourth), the hatchback profile was kept to delay boundary layer separation. It is observed that hatchback vehicles with rear slant angles of more than 30° show the flow feature of the square back vehicle. Considering the passenger's comfort, the top surface was inclined at 15.5° and the bottom surface is inclined at 36° .

In all cases, it is found that there is a stagnation point at the front surface where air hits the front face of the bus and wake at the rear of the bus. But with the modification in existing design wake formation is reduced somehow at the rear end of the second, third, and fourth models as shown in the above table. Velocity distribution at the bus body is almost zero and there is some acceleration over the surface of the bus which can be visualized in the above pictures.

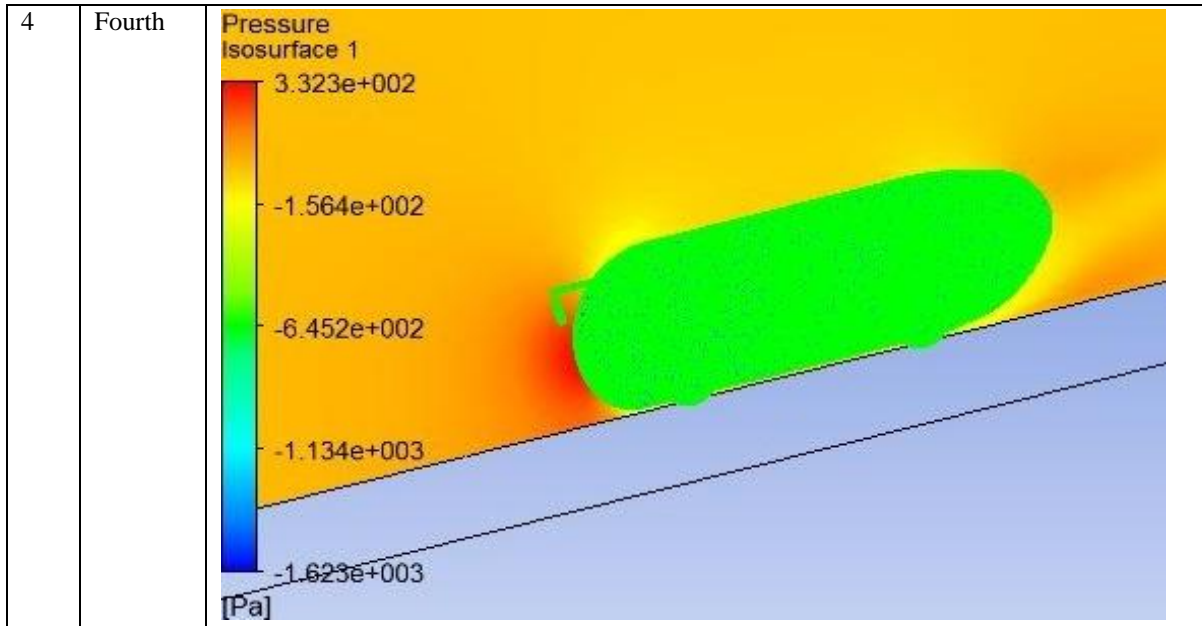
Pressure test

The movement of a bus at high speed creates a low-pressure region at the rear and high pressure at the front surface. The rear region creates a suctioning effect that tries to pull the vehicle backward due to wake formation at the rear. This aids further increasing the drag. Therefore, decreasing the size of the separation zone is a crucial aspect while considering to reduce drag.

The contour of pressure for existing and modified models are shown in the following table:

Table 6 Contour of the pressure of different bus models

| S.N | Model | Contour of pressure |
|-----|----------|---------------------|
| 1 | Existing | |
| 2 | Second | |
| 3 | Third | |



From the above pressure contour, it has been found that there is high-pressure distribution at the front surface and low pressure at the rear. The pressure difference of 249.473 Pa is found from the analysis of the existing model. The front, as well as back face of modified models, have been comparatively tapered to reduce the separation zone for reducing pressure difference in front and back end and the result shows that there is a reduction in pressure difference. The fourth model gave a minimum pressure difference. The values of pressure for the existing and fourth models are shown in the table below.

Table 7 Pressure distribution

| S.N | Model | Avg pressure at the front end | Avg pressure at the rear end | Pressure difference |
|-----|----------|-------------------------------|------------------------------|---------------------|
| 1. | Existing | 185.39 Pa | -64.083 Pa | 249.473Pa |
| 2. | Fourth | 174.48 Pa | -9.472 Pa | 183.956Pa |

From the above table, it can be seen that there is a reduction of the pressure difference between the front and rear surfaces in the fourth model compared to the existing model by 65.5 Pa. This reduction in pressure difference aids in reducing drag coefficient and thus drag force.

Streamlines

Streamlines around the bus body entering from velocity inlet and ending at the pressure outlet for the existing and fourth model are shown in the following table:

Table 8 Streamlines around bus model

| S.N | Model | Streamlines around the bus |
|-----|----------|----------------------------|
| 1 | Existing | |
| 2 | Fourth | |

Streamlines around the body for the fourth model are far better than the existing model. Streamlines of pressure entering at the front end of the bus, smoothly raising and running over the surface, and smoothly falling below the slanted rear surface can be seen in the above table.

From the analysis, the values of the drag coefficient of the existing model and new models were computed and compared. The computed drag coefficients were used to calculate the values of drag force for existing and all modified models. All values are plotted in the bar chart for comparison as follows:

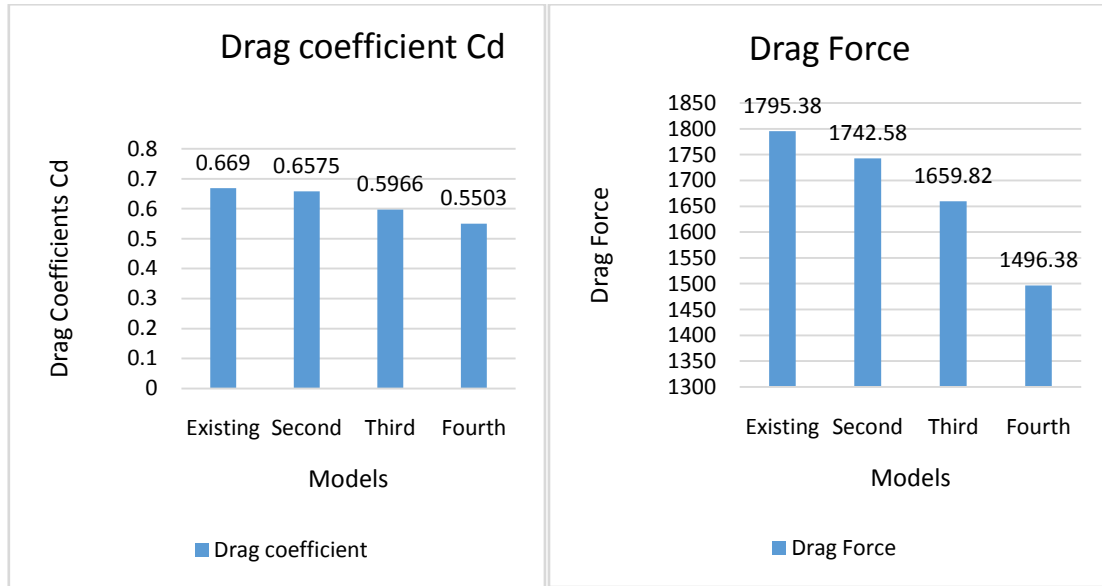


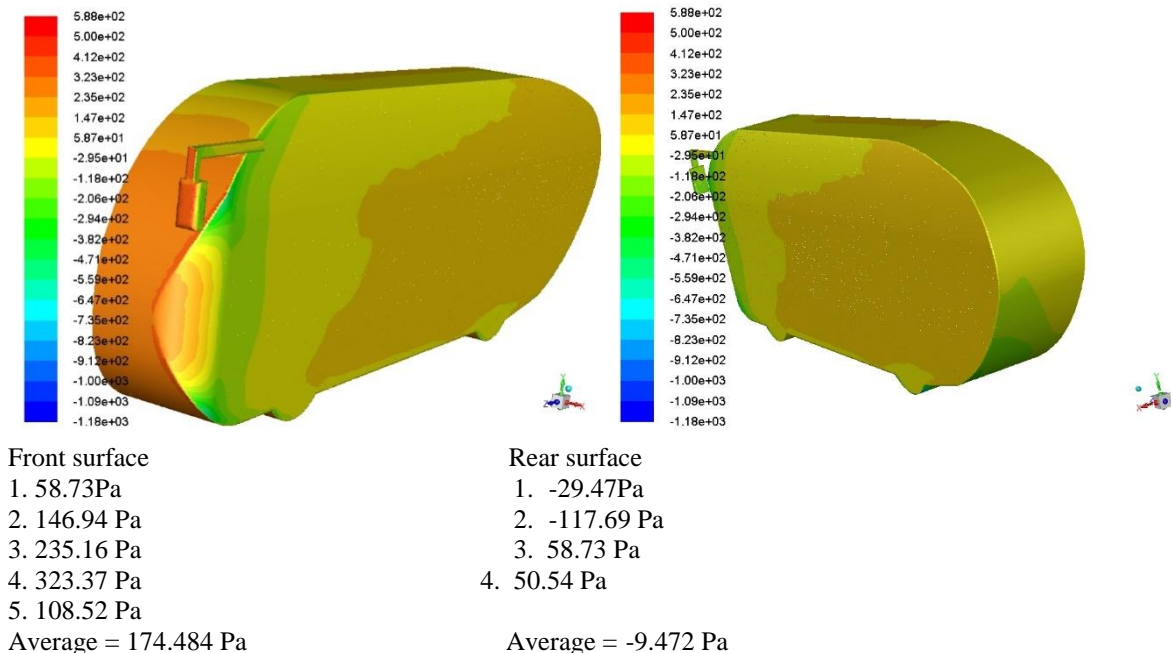
Figure 3 Comparison of drag coefficient and drag force for existing and modified models in the bar chart.

In the above chart, it can be seen that values are in descending order i.e. the drag coefficients, as well as drag force values, have gradually declined in modified models compared to an existing model. The drag coefficient of the Fourth model was decreased by 0.118 and the drag force was reduced by 300N as compared to the existing model.

Validation of the drag coefficient of the fourth model

The drag coefficient value for the fourth model was validated by comparing the results obtained from CFD analysis with hand calculation results.

Pressure distribution at the front and rear part of the fourth model is as follows:



Change in pressure(ΔP) = 174.484 – (-9.472)
 = 183.956Pa (against the motion of bus)

Pressure Drag Coefficient:

$$C_{dp} = \frac{\Delta P}{\rho * 0.5 * 22.22^2} = \frac{183.956}{1.225 * 0.5 * 22.22^2} = 0.608$$

Friction Drag Coefficient:

$$C_{df} = \frac{0.031}{Re^{\frac{1}{7}}}$$

$$C_{df} = \frac{0.031}{10.36}$$

$$C_{df} = 0.003$$

Total theoretical drag coefficient $C_d = 0.608 + 0.003 = 0.611$

Error in drag coefficient obtained from CFD analysis and hand calculation:

From simulation software, $C_d = 0.5508$

$$\begin{aligned} \%error &= \frac{0.611 - 0.5508}{0.661} * 100\% \\ &= 9\% \end{aligned}$$

Hence from the above calculation, the drag coefficient obtained from simulation software and hand calculation is similar. The percentage error was found to be below 10%.

Fuel consumption calculation and comparison:

Existing Model

Total drag force = 1795.38 N

Power required to overcome the drag force

$$= F * v$$

$$= 1795.38 * 22.22$$

$$= 39.89 \text{ KW}$$

Existing bus mileage = 5 km/ltr at 80 km/hr.

Indicated specific fuel consumption[9]:

$$= \frac{\text{mass of fuel consumed per hour}}{\text{indicated power of engine}} \dots \dots (5)$$

$$= \frac{V * \rho_f}{I.P}$$

$$= \frac{16 * 0.832}{140hp}$$

$$= 0.119 \text{ kg/KW hr.}$$

$$\text{Fuel consumption} = \frac{39.89 * 0.119}{0.832}$$

$$= 5.705 \text{ lt/hr.}$$

Modified(fourth) Model

Total drag force = 1496.38 N

Power required to overcome the drag force

$$= F * v$$

$$= 1496.38 * 22.22$$

$$= 33.249 \text{ KW}$$

Fuel consumption for the fourth model

$$= \frac{33.249 * 0.119}{0.832}$$

$$= 4.755 \text{ lt/hr}$$

From the above calculation, it can be found that the existing model requires 5.7 liters of fuel to overcome drag whereas the fourth model requires 4.75-liter fuel per hour i.e. approximately one-liter fuel can be saved for each 80km ride.

IV. CONCLUSION

A computational study was carried out to analyze the drag for 4 different bus models: one for the existing bus model and three modified models based on existing model dimensions. Results obtained were compared and the following points were concluded:

- The pressure difference between the front and rear surface of the bus was found to be 249.47 Pa and 183.95 Pa in the existing and fourth model respectively and it is reduced by 65.52 Pa due to the modified curved surface at the front and rear end of the bus.
- Due to the difference of pressure, the drag coefficient on the fourth model was reduced by 17.67% compared to the existing model.
- Fuel consumption declined by 16.65% in the fourth model as compared to the existing model hence, the fourth model is fuel-efficient than the existing model.

REFERENCES

- [1]. J. Lucas, "Live Science," 20 September 2014. [Online]. Available: <https://www.livescience.com>. [Accessed 10 January 2020].
- [2]. Rubel Chandra Dasa, "CFD Analysis of Passenger Vehicle at Various Angle of Rear End," Science Direct, 2017.
- [3]. R. Bhaskaran, "Black box," [Online]. Available: courses.edx.org. [Accessed Sunday, October 2019].
- [4]. N. R. B. H. YesfalgnDamissie, "Aerodynamic Drag Reduction on Locally Built Bus Body using Computational Fluid Dynamics (CFD)," *International Journal of Engineering Research & Technology (IJERT)*, vol. 6, no. 11, pp. 276-283, 2017.
- [5]. E. A. Mohamed, "Computational Investigation of Aerodynamic Characteristics and Drag Reduction of a Bus Model," *American Journal of Aerospace Engineering*, vol. 2, no. 1, p. 64, 2015.
- [6]. S. Thorat, G. Amba, and P. Rao, "Computational Analysis of Intercity Bus With Improved Aesthetics and Aerodynamic Performance on Indian Roads," *International Journal of Advanced Engineering Technology*, vol. 2, no. 3, pp. 103-109, 2011.
- [7]. E. A. Mohamed, "Computational Investigation of Aerodynamic Characteristics and Drag Reduction of a Bus Model," *American Journal of Aerospace Engineering*, vol. 2, no. 1, p. 64, 2015.
- [8]. M. Lanfrit, "Best practice guidelines for handling Automotive External Aerodynamics with FLUENT," *Fluent*, vol. 2, pp. 1-14, 2005.
- [9]. M. Bairwa, "Quora," 8 May 2017. [Online]. Available: <https://www.quora.com/What-is-specific-fuel-consumption..> [Accessed November 2019].

Kshitij Bhandari, et. al." Aerodynamics Simulation of PublicBusUsing CFD to reduce Drag and Fuel Consumption." *International Journal of Modern Engineering Research (IJMER)*, vol. 10(07), 2020, pp 05-17.